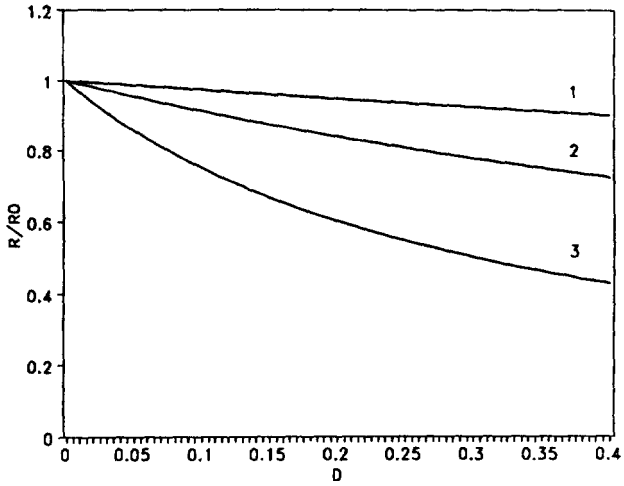

Figure 4. The ratio of R/R_0 for the bistable system with $\nu=0.2$. The curves 1, 2, and 3 correspond to $\mu=0.5$, $\mu=1$, and $\mu=2$, respectively.

and $\nu=0.9$, respectively. In Figure 4 we have taken μ to be 0.5, 1, and 2, respectively, when $\nu=0.2$. As D increases the ratio in large μ value decreases faster than the ratio in small μ does. As shown in Figure 3, it is obvious that in the region $\nu<1$ the transition rates decrease with increasing D. As the exponent ν increases, the transition rates decrease and relaxation times increase. In the limit $\nu\rightarrow1$, the transition rate approaches zero.

In the result, in the region for which $\nu<1$ the transition rates decrease as ν increases and ν decreases shown in Figure 3 and 4. However, in the case that $\nu>1$, it is obvious that in Eq. (17) never probability can be reach $y\rightarrow\infty$ in any finite time. It means that the system cannot be reach the unstable state since the concentration $x\rightarrow0$ (unstable point) corresponds to $y\rightarrow\infty$. When $\nu>1$ the random force is so weak that the system is entirely controlled by the deterministic term in the vicinity of the unstable state. The transition between the two deterministic stable states cannot occur and the initial distribution is continuously retained.

References

1. I. L'Hereux and R. Kapral, *J. Chem. Phys.* **88**, 1768 (1988).
2. C. Van den Broeck and P. Hnggi, *Phys. Rev.* **A30**, 2730 (1984).
3. J. M. Porra, J. Masoliver, and K. Lindenberg, *Phys. Rev.* **A44**, 4866 (1991); J. Masoliver, B. West, and K. Lindenberg, *ibid.*, **35**, 3086 (1987).
4. G. Hu and K. He, *Phys. Rev.* **A45**, 5447 (1992).
5. H. Risken, *The Fokker-Planck Equation*, Spinger-Velag, New York, 1984.
6. M. Kus, E. Wajnryb, and K. Wodkiewicz, *Phys. Rev.* **A43**, 4167 (1991).
7. P. Glansdorff and I. Prigogine, *Thermodynamic Theory of Structure, Stability, and Fluctuations*, Wiley-Interscience, New York, 1971.
8. R. J. Field and M. Burger, *Oscillations and Traveling Waves in Chemical Systems*, John Wiley & Sons, New York, 1974.
9. G. Nicolis and I. Prigogine, *Self-Organization in Non-equilibrium System*, John Wiley and Sons, New York, 1977.
10. F. Schlögl, *Z. Phys.* **248**, 446 (1971); **253**, 147 (1972).
11. C. J. Kim, D. J. Lee, and K. J. Shin, *Bull. Korean Chem. Soc.*, **11**, 557 (1990).
12. D. Chandler, *J. Chem. Phys.* **68**, 2959 (1978).
13. M. Abramowitz and I. A. Stegun, *Hanbook of Mathematical functions*, Natl. Bureau of Standards, 1965.
14. A. Nitzan, P. Ortoveva, J. Deutch, and J. Ross, *J. Chem. Phys.* **61**, 1056 (1974).
15. I. Procaccia and J. Ross, *J. Chem. Phys.* **67**, 5558 (1977).

Orbital Interactions in BeC_2H_2 and LiC_2H_2 Complexes

Ikchoon Lee* and Jae Young Choi

Department of Chemistry, Inha University, Inchon 402-751. *Received August 17, 1992*

Ab initio calculations are carried out at the 6-311G** level for the C_{2v} interactions of Be and Li atoms with acetylene molecule. The main contribution to the deep minima on the $^3B_2$ BeC_2H_2 and $^2B_2$ LiC_2H_2 potential energy curves is the b_2 $(2p(3b_2)-|\pi_g^*(4b_2))$ interaction, the a_1 $(2s(6a_1)-|\pi_u(5a_1))$ interaction playing a relatively minor role. The exo deflection of the C-H bonds is basically favored, as in the b_2 interaction, due to steric crowding between the metal and H atoms, but the strong in-phase orbital interaction, or mixing, of the a_1 symmetry hydrogen orbital with the $5a'_1$, $6a'_1$ and $7a'_1$ orbitals can cause a small endo deflection in the repulsive complexes. The Be complex is more stable than the Li complex due to the double occupancy of the 2*s* orbital in Be. The stability and structure of the MC_2H_2 complexes are in general determined by the occupancy of the singly occupied frontier orbitals.

Introduction

The interactions of metal atoms with molecules have been the subject of many experimental and theoretical studies.[1] The main purpose of the research in this field is a fundamental understanding of catalysis. It has been suggested that

for transition metals *V* through Ni the atomic 3*d* orbitals lie considerably below the 4*s* orbital and bonding in the catalyst system involves the 4*s* and 4*p* orbitals of the transition metals especially in the gas-phase catalysis on metal surfaces.[2,3a] Thus, as model theoretical studies, the bonding of a doubly occupied 2*s* and a companion, degenerate unoccupied, 2*p* orbitals of Be has been pursued. Several theoretical investigations on the interactions of Be atom with acetylene and ethylene have been carried out.[1,3] In the early works of Schaefer *et al*,[1a] and Witko *et al*,[1c] rigid hydrocarbon structures were assumed in the *ab initio* calculations on the Be-(or Mg) C_2H_2 and Be-$_2H_4$ systems. More recently Balaji and Jordan[1] have shown using the 6-31G* basis set on the interactions of Be and Mg atoms with C_2H_2 and C_2H_4 that distortions of the hydrocarbons are important for proper description of the interactions.

In this work, we examine the C_{2v} interactions of metal atoms(M), Be and Li, with acetylene molecule using the triple split basis set 6-311G**[4]. This basis set has the increased overall flexibility of the representation and provides a better description of the outer valence region especially for a system with H atoms, compared with the 6-31G* basis set, by splitting an outer valence region into three parts and supplementing a single set of uncontracted p-type gaussians for hydrogen. Moreover, in this basis set the electron correlation within the atomic valence region has been partially accounted for at the MP2 level.[4] The 6-311G** is, thus, much superior to the 6-31G* basis set for energy as well as structure comparison,[5] and we in fact find interesting different behaviors from those calculated with 6-31G*.[1]

Computational Detail

All calculations were performed using the Gaussian 86[6] and contour diagram and topographic pictures were drawn by the modified Monstergauss program.[7] The split valence (6-31G), polarized split valence (6-31G*), triple split valence (6-311G) and polarized triple split valence (6-311G* and 6-311G**)[4] contracted Gaussian basis sets were used in the RHF, UHF and electron correlation of frozen-core CISD and MP4 calculations.[4] All geometries, for ground states and exciplexes, were fully optimized with conservation of their electronic states by the direct energy minimization routine.[6]

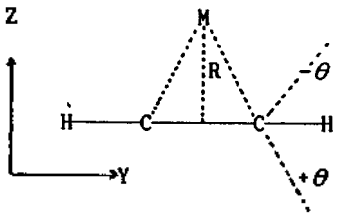

In the metal atom -C_2H_2 interacting system, the metal atom (Be or Li) approaches along the perpendicular bisector of the C≡C bond at a distance R between the metal atom(M) and mid-point of C≡C. The M-C_2H_2 system is coplanar within the *YZ* plane. In the optimization of M-C_2H_2 complexes, the geometry of C_2H_2 is relaxed and the C_{2v} distortions are allowed with an endo (−θ) or exo (+θ) deflection.

Results and Discussion

Total energies and ionization potentials of Be(^{1}S), Be$^+$(^{2}S) and Be(^{3}P), and those of Li(^{2}S), Li$^+$(^{1}S) and Li(^{2}P) at various levels of theory are reported in Tables 1 and 2. Similarly the structures, total energies and ionization potentials of the C_2H_2 molecule are given in Table 3. Since the second superscript star denotes basis set supplemented by a single set of p-type gaussian function for hydrogen,[4] the results of 6-311G* and 6-311G** calculations are the same for heavy atoms (Be and Li). We note that the effect of basis sets used is small on the structure but is relatively large on the

Table 1. Total Energy and Ionization Potential of Be Atom at Various Levels of Approximation

Basis set	Be(^1S) total energy[a]	I.P.[b]	Be$^+$(^2S) total energy[a]	I.P.[b]	Be(^3P) total energy[a]	I.P.[b]
6-31G	−14.566764	0.30130	−14.275410	0.66570	−14.506550	0.23699
6-31G*	−14.566944	0.30154	−14.275520	0.66578	−14.507843	0.23956
6-311G	−14.571873	0.30886	−14.276195	0.66590	−14.510331	0.24140
6-311G*	−14.571873	0.30886	−14.276195	0.66590	−14.511977	0.24465
CISD/6-311G*	−14.631848	0.30886	−14.276195	0.66590	−14.515886	0.24465
MP4/6-311G*	−14.637093	0.30886	−14.276195	0.66590	−14.515886	0.24465

[a]Total energy(a.u.). [b]Ionization potential(a.u.)

Table 2. Total Energy and Ionization Potential of the Li Atom at Various Levels of Approximation

Basis set	Li(^1S) total energy[a]	I.P.[b]	Li$^+$(^2S) total energy[a]	I.P.[b]	Li(^3P) total energy[a]	I.P.[b]
6-31G	−7.431235	0.19576	−7.235480	2.79256	−7.360051	0.12459
6-31G*	−7.431372	0.19585	−7.235536	2.79176	−7.360104	0.12459
6-311G	−7.432026	0.19622	−7.235838	2.79239	−7.364233	0.12842
6-311G*	−7.432026	0.19622	−7.235838	2.79239	−7.364238	0.12843

[a]Total energy(a.u.). [b]Ionization potential(a.u.).

Table 3. Total Energy, Ionization potential, and Structure of Acetylene at Various Levels of Approximation

	Total energy (a.u.)	$^1C_2H_2$ I.P.(a.u.)	Structure[a]		Total energy		$^3C_2H_2$ C-C	Structure[b]	
			C-C	C-H	(a.u)	(a.u)		C-H	(C-C-H)
6-31G	−76.792762	0.40703	1.194	1.053	−76.691145	0.36429	1.319	1.079	129.5
6-311G	−76.811434	0.41267	1.187	1.050	−76.705890	0.36934	1.323	1.077	129.6
6-31G*	−76.821837	0.40446	1.186	1.056	−76.724156	0.36697	1.315	1.080	128.7
6-311G*	−76.835143	0.41268	1.182	1.055	−76.736449	0.37341	1.315	1.098	128.4
6-311G**	−76.841237	0.41325	1.182	1.055	−76.740484	0.37234	1.315	1.080	128.7
CISD/6-311G**	−77.127226	0.41325	1.182	1.055	−76.979939	0.37234	1.315	1.080	128.7
MP4/6-311G**	−77.137332	0.41325	1.182	1.055	−76.995398	0.37234	1.315	1.080	128.7

[a] Linear type. [b] *cis* type.

energetics. For the ground state C_2H_2, the total energy difference between 6-31G* and 6-311G** is 12.17 kcal/mol, which is further lowered by the use of MP4/6-311G** by 185.87 kcal/mol. This indicates that electron correlation effect is significant for C_2H_2 and in this respect the use of 6-311G** is expected to provide a better description of MC_2H_2 complexes compared to 6-31G*.

Orbital Interactions[6]. Orbital and state (in parenthesis) symmetries of the metal (Be) atom, C_2H_2 molecule and the C_{2v} BeC_2H_2 complex at two arbitrary distances(R) of weakly (R≥4.5 Å) and strongly (R≅2.0 Å) interacting systems are schematically presented in Figure 1. In this Figure, the electronic configuration and orbital correlations are shown for the $^3B_2$ BeC_2H_2 exciplex, in which one 2*s* electron is excited to 2p_y orbital ($6a_1 \rightarrow 3b_2$). Likewise, other states are obtaineed by exciting a 2*s* electron into different 2*p* levels; $2s \rightarrow 2p_x (6a_1 \rightarrow 2b_1)$ and $2s \rightarrow 2p_z$ ($6a_1 \rightarrow 7a_1$) give $^3B_1$ and $^3A_1$ BeC_2H_2 exiplexes, respectively. As the two species, *i.e.*, the metal atom and C_2H_2, approach, the weak perturbation at a relatively long distance causes to split the degenerate 2*p* and π_u (and π_g^*) levels. At a shorter distance, orbital interactions between the same symmetry species grow stronger (resulting orbitals are designated with a prime symbol). The following three types of symmetry allowed interactions are envisaged.

The a_1 Type Interaction. Reference to Figure 1 reveals that the a_1 symmetry-adapted orbital, (closed shell) $5a_1$ ($1\pi_u$), of C_2H_2 can interact with the $6a_1$ (2*s*) and $7a_1$(2p_z) orbitals of the metal atom, and results in three a_1 orbitals, $5a_1'$, $6a_1'$ and $7a_1'$, of the MC_2H_2 complexes at short M-C_2H_2 distances. In this three-orbital interaction, donation of electron takes place from the doubly occupied 1 π_u of C_2H_2 to empty or partially empty orbitals of 2*s* and 2p_z of the metal atom. The resulting orbital shapes of $5a_1'$ and $6a_1'$ are schematically shown below, and a contour diagram and topographic

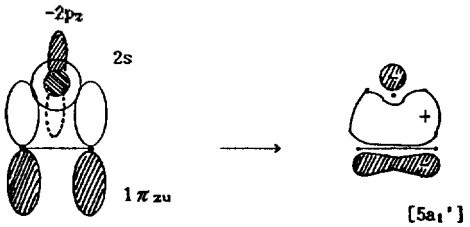

$$\psi(5a_1') = C_{a1}\phi(1\pi_{zu}) + C_{a2}\phi(2s) - C_{a3}\phi(2p_z)$$
$$\text{with } C_{a2} > C_{a3}$$

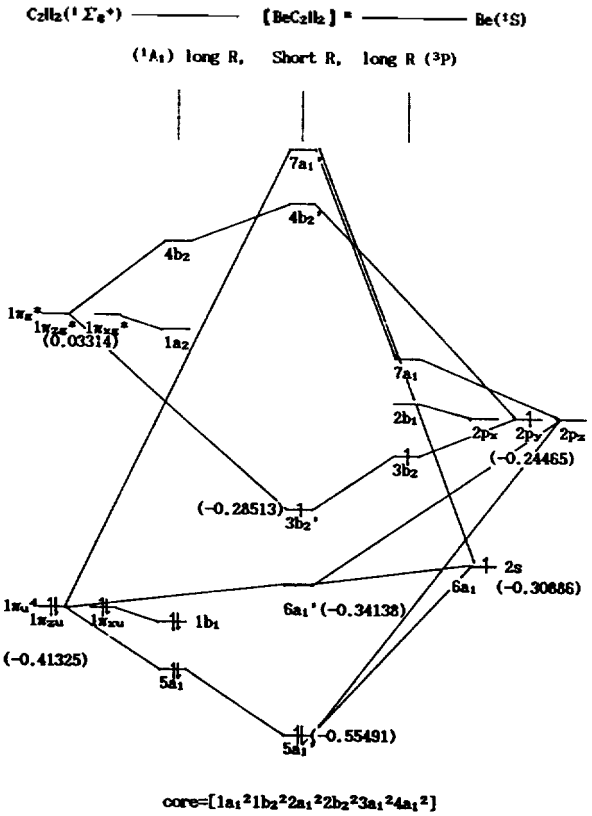

core=[$1a_1^2 1b_2^2 2a_1^2 2b_2^2 3a_1^2 4a_1^2$]

Figure 1. The electron configuration and orbital interactions as Be approaches C_2H_2 to form a C_{2v} complex $^3B_2$ BeC_2H_2. Orbital and state (in parenthesis) symmetries are shown. The relevant orbital energies are given in hartrees.

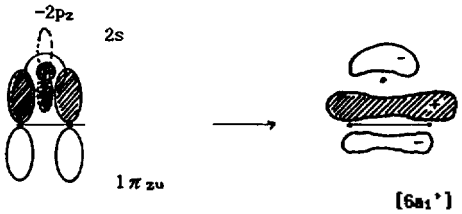

$$\psi(6a_1') = C_{a1}'\phi(1\pi_{zu}) - \{C_{a2}'\phi(2s) + C_{a3}'\phi(2p_z)\}$$
$$\text{with } C_{a2}' > C_{a3}'$$

view of $6a_1'$ are presented in Figures 2*s* and 2*b*, respectively. These orbital shapes and contour diagram demonstrate the

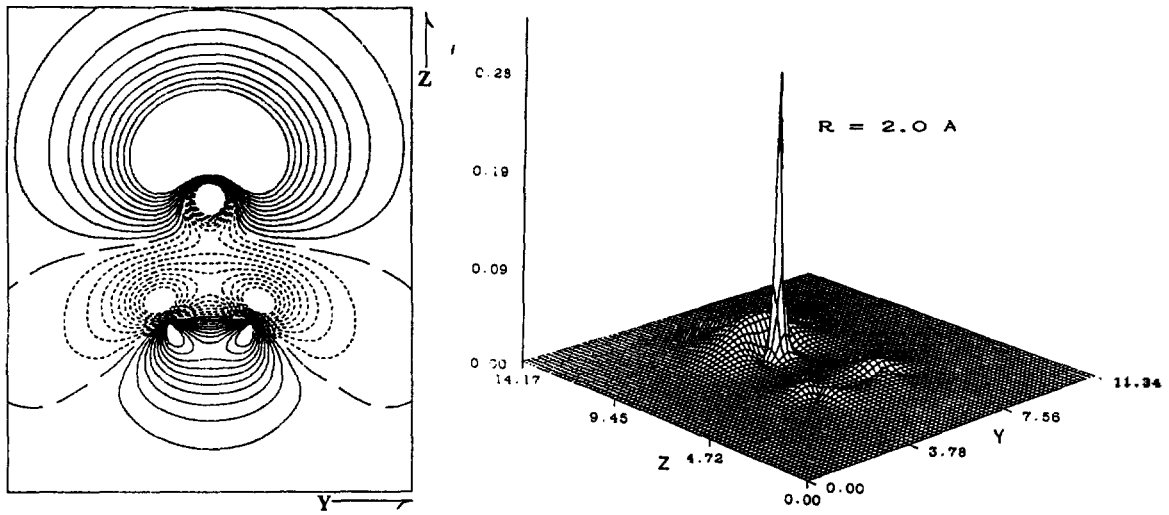

(a) (b)

Figure 2. Contour diagram (a) and topographic picture (b) of the $6a_1$ orbital of $^3B_2$ BeC_2H_2.

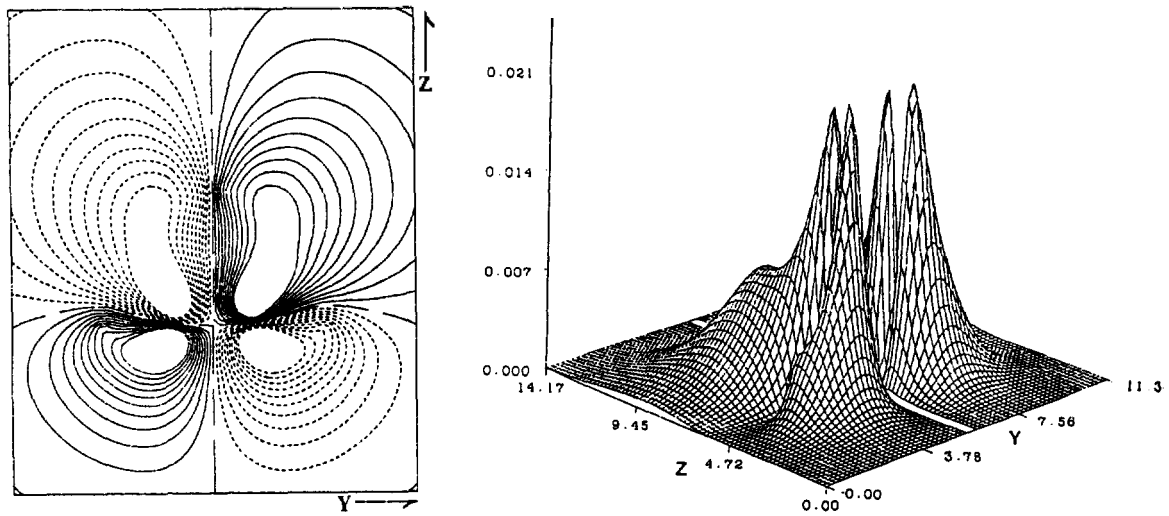

(a) (b)

Figure 3. Contour diagram (a) and topographic picture (b) of the $3b_2'$ orbital of $^2B_2$ LiC_2H_2.

strong and weak bonding nature of the two orbitals, $5a_1'$, and $6a_1'$, respectively. Hence, electron occupation of these orbitals will lead to a strong ($5a_1'$) and weak ($6a_1'$) bonding between M and C_2H_2 and hence results in stabilization of the MC_2H_2 complex. We note in Fig. 2(a) that the mixing-in of $2p_z$ is smaller than that of 2_s due to larger energy gap between $1\pi_u$ and $2p_z$ than that between $1\pi_u$ and $2s$, and hence the coefficient C_{a2}' is greater than C_{a3}'.

The b_2 Type Interaction. There are two b_2 orbitals, one each in C_2H_2 ($1\pi_g^* \rightarrow 4b_2$) and metal ($2p_y \rightarrow 3b_2$), which can interact to form a pair of new orbitals, $3b_2'$, and $4b_2'$, in the MC_2H_2 complex at short M-C_2H_2 distance. The lower of these, $3b_2'$, is a relatively strong bonding orbital, as can be seen from the schematic orbital shape, [$3b_2'$], and a contour diagram and topolographic view in Figures 3(a) and 3(b), respectively. The bonding character of this [$3b_2'$], is stronger than that of [$6a_1'$] but is weaker than that of [$5a_1'$]. An electron in the metal-atom p_y orbital will be back-donated

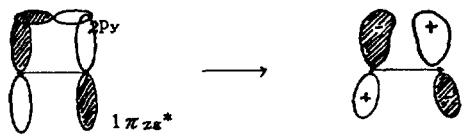

[$3b_2'$]

$$\psi(3b_2') = C_{b1}\phi(1\pi^*_{zg}) + C_{b2}\phi(2p_y)$$

to the empty acetylene $1\pi_g^*$ orbital due to the [$3b_2'$] type of overlap (Figures. 3(a) and 3(b)).

The b_1 Type Interaction. Again, there are two b_1 symmetry-adapted orbitals, one each in C_2H_2 ($1\pi_u \rightarrow 1\ b_1$) and metal atom ($2p_x \rightarrow 2b_1$). The interaction at short M-C_2H_2 distance will lead to the two new MO's one stabilizing, $1b_1'$, and the other, destabilizing, $2b_1'$. The MO's are within the XY plane so that they are perpendicular to the other MO's formed by a_1 and b_2 type interactions. The overlap of the two b_1 orbitals is, however, smaller than that of the b_2 type

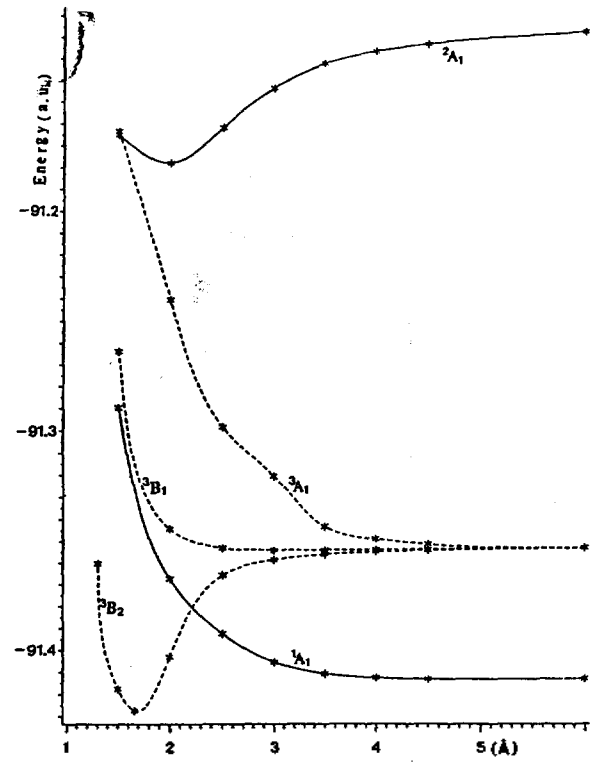

Figure 4. Potential energy curves for the Be-C_2H_2 system at the 6-311G** level.

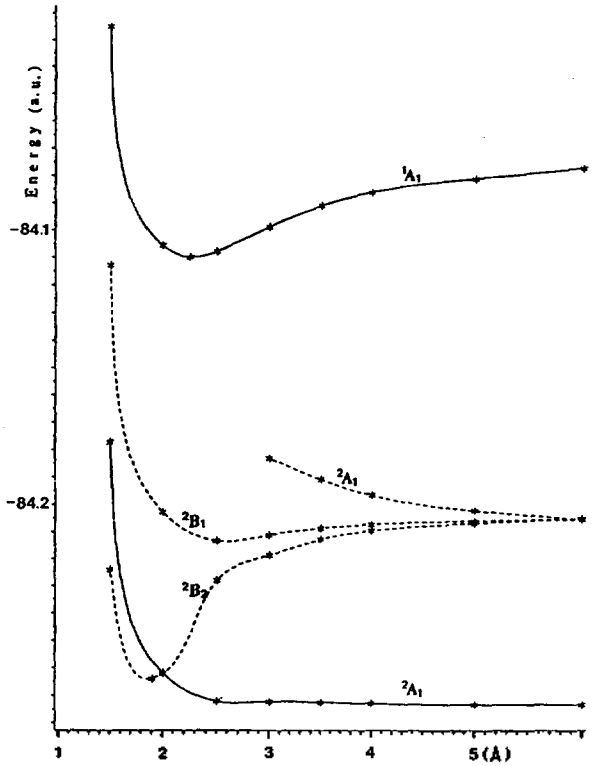

Figure 5. Potential energy curves for the Li-C_2H_2 system at the 6-311G** level.

interaction, especially at short M-C_2H_2 distance. This means that the stabilization of the MC_2H_2 complex due to electron occupation of the $1b_1'$ orbital is less compared to that of the $3b_2'$ orbital. The energy stabilization incurred to the MC_2H_2 complex by the same occupation number (1 or 2 electron) at the same M-C_2H_2 distance, R, will therefore decrease in the order, $5a_1'>3b_2'>1b_1'>6a_1'$. However, in accordance with the frontier orbital(FMO) theory,[9] the critical orbitals in determining stability and structure of the MC_2H_2 complexes will be the highest occupied (HOMO) $3b_2'$, $1b_1'$, and $6a_1'$, which is in most cases singly occupied (SOMO). We therefore focussed our discussion upon the role of these SOMOs[10] playing in particular in controlling the complex stability and structure.

Potential Energy Curve and Structure. Theoretical potential energy curves calculated at the 6-311G** level for the approach of the metal atom(M) toward an acetylene molecule forming a C_{2v} MC_2H_2 system is presented in Figures 4 and 5 for M=Be and Li respectively. We have allowed specification of occupation numbers according to the symmetry types in the ground state potential energy curve calculations using symmetry-adapted orbitals in the SCF program. This means that the electronic configurations are kept to $\cdots 5a_1^2 1b_1^2 6a_1^2$ and $\cdots 5a_1^2 1b_1^2 6a_1$ for the ground state $^1A_1$ BeC_2H_2 and $^2A_1$ LiC_2H_2 respectively. The two ground state curves in Figures 4 and 5 indicate that the ground states are both repulsive, at short M-C_2H_2 distances provided the electronic configurations are conserved. If we relax this condition of specifying occupation numbers, a stable state $^1A_1$ BeC_2H_2 appears with the electronic configuration of $\cdots 5a_1^2 1b_1^2 3b_2^2$ which is an exciplex formed by the excitation of two $6a_1$ ($2s$) electrons to $3b_2$ ($2p_y$) level.[1] We hve not considered this type of exciplex in this work. However, we can easily account for this stable $^1A_1$ complex, since the occupation of the $3b_2'$ level by two electrons will certainly be favored relative to the double occupancy of the $6a_1'$ level, as we stressed in the discussion of orbital interactions above.

Another important factor contributing to the stability attained by the occupation of $3b_2'$ insteau of $6a_1'$ is the release of steric repulsion between the approaching metal atom and the two hydrogen atoms. The steric repulsion and hence destabilizing energy of the MC_2H_2 complex should increase or decrease depending on whether the C-H bonds deflect toward ($-\theta$, endo deflection) or away from ($+\theta$, exo deflection) the approaching metal atom. Simple orbital mixing concept shows that in the $6a_1'$ (and $5a_1'$) orbital the two hydrogens exhibit endo deflection whereas in the $3b_2'$ orbital they form exo conformation. The two hydrogen atoms can have either a_1 (H_1+H_2) or b_2 (H_1-H_2) symmetry species. The a_1 symmetry species of hydrogen orbitals will mix-in and overlap in-phase with the positive sign electron clouds between M and C_2H_2 of $6a_1'$ (and also of $5a_1'$ and $7a_1'$) orbital, [I], so that the C-H bonds deflect in endo($-\theta$) fashion (in all a_1 interactions); in contrast the b_2 symmetry hydrogen orbitals overlap in-phase with the two lobes extending away from the M-C_2 region of the $3b_2'$ orbital, [II], resulting in

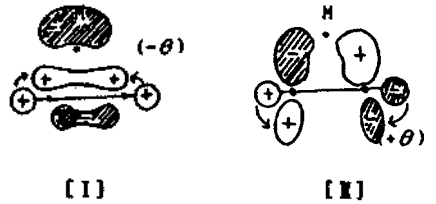

[I] [II]

Table 4. Structures and Dissociation Energies of the Stable Complexs by the 6-311G** Basis Set

Complex	$^2A_1$ $BeC_2H_2^+$	$^3B_2$ BeC_2H_2
Total energy(a.u.)	−91.178332[d]	−91.427209[d]
Distance R(Å)	2.032[a]	1.771[a]
	1.952[d]	1.657[d]
Dissociation	30.00[a]	19.10[a]
Energy(kcal/mol)	40.81[b]	49.12[b]
	—	61.57[c]
	38.06[d]	46.43[d]
	44.22[e]	58.96[e]
	44.22[f]	59.30[f]
Structure[d]	1.195 Å (C-C)	1.255 Å (C-C),
cis type	1.067 Å (C-H)	1.071 Å (C-H),
	3.49° (C-C-H)	30.32 (C-C-H)

[a]Ref. 3(a); [b]Ref. 1, at 6-31G* level; [c]Ref. 1, at MP2/6-31G* level; [d]This work at 6-311G** level; [e]This work at CISD/6-311G** level; [f]This work at MP4/6-311G** level.

an exo deflection (+θ).[11] Thus the endo deflection should increase the steric repulsion energy whereas in the exo-form the steric repulsion is released. These steric energy changes must be considered additionally to the energy changes due to orbital lowering. The distortion of the C-H bonds brings further energy lowering for the occuption of the $3b_2'$ level but causes energy destabilization for the occupation of the $6a_1'$ orbital. Since the endo (−θ) deflection is sterically unfavorable in contrast to the sterically favorable exo (+θ) deflection, the magnitude of actual deflection, θ, will be small in the endo but it will be large in the exo deflection.

There is no b_1 symmetry hydrogen orbital so that the electron occupation of $1b_1'$ MO has no effect on the C-H bond distortion.

The endo type deflection was not found by Balaji *et al.*[1], even through they allowed geometry distortions in their optimizations using the 6-31G* basis set. They also found that the exo deflection stabilizes the $3b_2'$ orbital, but the reason behind this stabilization due to distortion i.e., the in-phase mixing or overlap of the hydrogen b_2 orbital, was not discussed. We believe that the use of the better basis sets, 6-311G** rather than 6-31G*, helped to demonstrate subtle geometrical changes involving hydrogen atoms in a greater detail[5] than it was possible in the previous work of Balaji *et al.*[1]

$^2A_1$ $BeC_2H_2^+$. Ionizing one electron from Be 2*s* ($6a_1$) orbital results in an electron configuration of this state $\cdots 5a_1^2 1b_1^2 6a_1$. This cationic complex should have only weak orbital stabilization energy, but the potential energy curve, Figure 2, has a minimum corresponding to a stable complex at $R=2.032$ Å. The dissociation energy of this complex is 38.06 kcal/mol, which is greater by ~8 kcal/mol than that of rigid complex[3a] but is lower by 2.70 kcal/mol than that calculated with 6-31G*[1] (Table 4). The stability of this complex is considered mostly due to electrostatic interaction.[1,3a] The stable cationic complexis important in the solution phase catalysis, since in the solution the catalysist metals exist in cationic forms which are stabilized by solvation.

$^1A_1$ BeC_2H_2. This state has an electronic configuration of $\cdots 5a_1^2 1b_1^2 6a_1^2$, and has a repulsive potential energy curve (Figure 2) at all Be-C_2H_2 distances. It exhibited a small endo deflection ($\theta=-3.5°$) at $R=2.0$ Å due to double occupation of $6a_1'$. Another $^1A_1$ state with $\cdots 5a_1^2 1b_1^2 3b_2^2$ configuration has been reported to show a deep minimum[1], which is most certainly due to double occupation of $3b_2'$ instead of $6a_1'$.

$^3A_1$ BeC_2H_2. This state with $\cdots 5a_1^2 1b_2^2 6a_1 7a_1$ configuration has also a repulsive potential energy curve at all distance (R). At a shorter distance, $R=2.0$ Å, the C-H bond stretches to an abnormally long distance of 1.270 Å with an endo deflection of $\theta=-7.4°$ due to an electron in highly antibonding $7a_1'$. Here again the occupation of $6a_1'$ and $7a_1'$ causes not only an endo deflection of the C-H bonds but also a repulsive, unstable, state.

$^3B_2$ BeC_2H_2. This state with an electronic configuration of $\cdots 5a_1^2 6a_2 3b_2$ has an energy minimum in the potential energy curve. The stable complex is formed at $R=1.657$ Å with the dissociation energy of 46.43 kcal/mol (Figure 2). Reference to Table 4 reveals again that the dissociation energy is much greater than that calculated by a rigid model,[3a] but is smaller by 2.7 kcal/mol than that calculated by 6-31G*.[1] The energy difference of 2.7 kcal/mol is exactly the same amount that was found for $^2A_1$ $BeC_2H_2^+$ above. Similarly our frozen-core MP4 result (with 6-311G**) of the dissociation energy is lower by 2.3 kcal/mol than the corresponding value by 6-31G*[1]; this demonstrates clearly a tendency of over-estimation for the complex stability by 6-31G* relative to 6-311G**.

The stable complex at the energy minimum has a large exo deflection of the C-H bonds ($\theta=+30.3°$) due to the occupation of the moderately bonding $2b_2'$ which is accompanied by a release in steric repulsion energy.

$^3B_1$ BeC_2H_2. This state with an electron configuration of $\cdots 5a_1^2 1b_1^2 6a_1 2b_1$ is repulsive at short Be-C_2H_2 distances (Figure 4). The two singly occupied orbitals, $6a_1$ and $2b_1$, will be bonding at short distances R, but the occupation of $6a_1$ causes a small endo deflection ($\theta=-2.6°$) at $R=2.0$ Å; the increase in steric repulsion due to this endo deflection at short distance R appears to cancel out and indeed exceed the stability gained by the orbital lowering. The occupancy of $2b_1$ orbital has no effect on the C-H bond distortion.

$^2A_1$ LiC_2H_2. For this ground state with an electron configuration of $\cdots 5a_1^2 1b_1^2 6a_1$, the potential energy curve shows no stable species (Figure 5). The C-H bonds exhibit endo deflection ($\theta=-4.5°$) at $R=2.0$ Å, which is as expected for the states with occupation of the $6a_1'$ level.

$^1A_1$ $LiC_2H_2^+$. This state has an electron configuration of $\cdots 5a_1^2 1b_1^2$ and has a stable form at $R=2.253$ Å with the dissociation energy of 20.97 kcal/mol (Table 5). The stability

Table 5. Structures and Dissociation Energies of the Stable Complexes at the 6-311G** Level

Complex	Distance(Å)	Dissociation energy	Structure		
	R	(kcal/mol)	C-C(Å)	C-H(Å)	C-C-H(θ)
$^1A_1$ $[Li\text{-}C_2H_2]^+$	2.253	20.97	1.189	1.062	4.55
$^2B_1$ $[Li\text{-}C_2H_2]$	2.512	5.15	1.184	1.058	2.22
$^2B_2$ $[Li\text{-}C_2H_2]$	1.890	36.81	1.266	1.078	40.08

of this cationic species originates mainly from electrostatic interaction[1,3a], albeit the stabilized $5a_1'$ and $1b_1$ levels are doubly occupied. The C-H bonds show small exo deflection ($\theta = +4.5°$) which may results from electrostatic repulsion between Li^+ and the two H atoms.

$^2A_1$ LiC_2H_2. This state has an electron excited from $2s$ ($6a_1$) to $2p$ ($7a_1$) level, $\cdots 5a_1^2 1b_1^2 7a_1$. However this state disappears at a closer distance, $R<3.0$ Å, due to orbital jump of the $7a_1$ electron back to the $6a_1$ level *i.e.*, back to the $^2A_1$ ground state (Figure 5).

$^2B_1$ LiC_2H_2. This state having an electron configuration of $\cdots 5a_1^2 1b_1^2 2b_1$ shows a shallow minimum with the dissociation energy of 5.0 kcal/mol on the potential energy curve, Figure 5, at $R=2.512$ Å. Energy stabilization due to the occupation of $1b_1'$ level will not be large, but on the other hand there is no adverse effect of increasing steric repulsion between the Li atom and the two H atoms as the distance R decreases (vide supra). Thus the C-H bonds show very little exo deflection ($\theta = +2.2°$), alleviating the increase in steric repulsion.

$^2B_2$ LiC_2H_2. This exciplex formed by exciting a $2s$ ($6a_1$) electron to $2p_y$ ($3b_2$) level ($\cdots 5a_1^2 1b_1^2 3b_2$) has a relatively deep minimum on the potential energy curve at $R=1.890$ Å with the dissociation energy of 36.81 kcal/mol (Table 5). As expected from occupancy of $3b_2'$ level, the C-H bonds show a large exo deflection, $\theta = +40.8°$. This is a greater exo deflection than the corresponding one in $^3B_2$ BeC_2H_2, in which an electron in $6a_1'$ causes a small endo deflection. The stability of the complex is ca. 10 kcal/mol less than the corresponding state of Be complex, $^3B_2$ BeC_2H_2, in which an additional electron in the $6a_1'$ level will, no doubt provide an additional energy stabilization. Thus comparing the two metal atoms with double (Be) and single (Li) occupancy of the $2s$ level, the former with closed shell $2s$ orbital leads to a greater stability of MC_2H_2 complex. Extending the analogy to the transition metals, we may conclude that the atoms with the closed shell $4s$ and empty $4p$ are better catalysts than the atoms with the partially occupied $4s$ (and $4p$) orbital.

Conclusions

Three types of symmetry allowed orbital interactions, a_1, b_1 and b_2, are possible in the metal atom (Be and Li)-acetylene systems. The b_2 interaction allows back-donation of $2p$ metal-atom electron into vacent $1\pi_g^*$ C_2H_2 orbital, providing a greatest orbital stabilization as well as a release in the steric repulsion rendered by an exo deflection of the C-H bonds. In the a_1 type three-orbital interaction, electron is donated from $1\pi_u$ C_2H_2 orbital to the $2s$ metal-atom orbital leading to a moderate orbital stabilization, which is, however, accompanied by an adverse steric repulsion effect due to an endo deflection of the C-H bonds. As a result, stable complexes are formed only in the b_2 interactions, $^3B_2$ BeC_2H_2 and $^2B_2$ LiC_2H_2, in contrast to the repulsive potential energy curves in the a_1 interactions, $^3A_1$ BeC_2H_2 and $^2A_1$ LiC_2H_2. The C-H bond distortion is not symmetry allowed in the b_1 interaction so that a very weakly bound complex is obtained with $^2B_1$ LiC_2H_2 state. The stability and structure of the MC_2H_2 complexes can be accounted for in general by considering only the occupancy of the singly occupied (SOMO) orbitals in accordance with the FMO theory.

Acknowledgement. Major part of calculations was done at Department of Chemistry, University of Saskachewan. One of us (J.Y.C) thanks Drs. J. Pipek, P. G. Mezey and O. P. Strausz for their valuable discussion and hospitality.

Reference

1. V. Balaji and K. D. Jordan, *J. Phys. Chem.*, **92**, 3101 (1988) and references cited therein.
2. E. Clementi and C. Roetti, *At. Data Nucl Data Tables*, **14**, 177 (1974).
3. (a) W. C. Swope and H. F. Schafer, *J. Am. Chem. Soc.*, **98**, 7962 (1976); (b) R. K. Gosavi, O. P. Strausz, F. Bernadi, A. Karper and P. G. Mezey, *J. Phys. Chem.* **91**, 283 (1987); (c) M. Witko and V. Bonacic-Koutecky, *Int. J. Quant. Chem.*, **29**, 1535 (1986).
4. W. J. Hehre, L. Radom, P. V. R. Schleyer, and J. A. Pople, *Ab initio Molecular Orbital Theory*, Wiley, New York, 1986, Chapter 4.
5. (a) K. B. Wiberg and K. E. Laidig, *J. Am. Chem. Soc.*, **109**, 5935 (1987); (b) J. E. Del Bene, D. H. Aue and I. Shavitt, *J. Am. Chem. Soc.*, **114**, 1631 (1992).
6. M. J. Frisch, J. S. Binkley, H. B. Schlegel, K. Raghawachari, C. F. Melius, R. L. Martin, J. J. P. Stewart, F. W. Brobrowicz, C. M. Rohlfing L. R. Kahn, D. J. DeFrees, R. Seager, R. A. Whiteside, D. J. Fox, E. M. Fleuder, and J. A. Pople, GAUSSIAN 86, Carnegi-Mellon Quantum Chemistry Publishing Unit, Pittsburgh, PA, USA, 1986
7. M. Peterson and R. Poirier, Monstergauss Program, Chemistry Dept., University of Tronto, Toronto, Canada, June 1981.
8. T. A. Albright, J. K. Burdett, and M. H. Whangbo, *Orbital Interactions in Chemistry*, Wiley, New, York, 1985.
9. (a) K. Fukui, T. Yonezawa, and H. Singu, *J. Chem. Phys.*, **20**, 722 (1952); (b) I. Fleming, *Frontier Orbitals and Organic Chemical Reactions. Wiley*, New York, 1976; (c) K. Fukui, *Theory of Orientation and Stereoselection*, Springer-Verlag, Berlin, 1975.
10. (a) L. Salem, *J. Am. Chem. Soc.*, **90**, 543 (1968); (b) L. Salem, *Electrons in Chemical Reactions. First Principles*, Wiley New York, 1982, Chapter 6.
11. The endo deflection may result by mixing in of the b_2 hydrogen orbital to $3b_2'$ if signs are exchanged (corresponding to mixing-in with a sign reversal), but this is sterically disfavored way of mixing.